JOURNAL OF GEOPHYSICAL RESEARCH, VOL. 111, B12S09, doi:10.1029/2006JB004499, 2006

Day plots of mixtures of superparamagnetic, single-domain, pseudosingle-domain, and multidomain magnetites

David J. Dunlop[1] and Brian Carter-Stiglitz[2]

Received 11 May 2006; revised 28 July 2006; accepted 30 August 2006; published 14 November 2006.

[1] We test how well a few hysteresis parameters (saturation remanence M_{rs}, coercive force H_c and remanent coercivity H_{cr}) serve to determine the proportions of end-members in binary mixtures. Our end-members are six magnetites whose grain sizes are within the superparamagnetic (SP), stable single-domain (SD, three samples), pseudo-SD (PSD), and multidomain (MD) ranges (Carter-Stiglitz et al., 2001). The three SD magnetites have contrasting origins and properties: (1) bacterial magnetite crystals of a single size and coercivity, arranged in chains; (2) natural volcanic magnetites with a narrow distribution of coercivities; and (3) synthetic magnetites precipitated in glass, with a broader coercivity distribution. Our parameter mixing theory assumes linear magnetization curves of the end-members between zero field and the largest coercive force H_c (that of the SD phase, if present). Similarly remanent hysteresis curves should be linear up to the maximum remanent coercive force H_{cr}. Three of our mixtures (SP plus bacterial SD, PSD plus bacterial SD, MD plus volcanic SD) had acceptable agreement between predicted and measured dependences of H_c, H_{cr} and the curve of M_{rs}/M_s versus. H_{cr}/H_c (Day plot) on end-member concentrations. A nonlinear approximation to remanent hysteresis curves gave a reasonable fit to MD plus glass SD results. In this case, H_{cr}/H_c for the most MD-rich mixture is larger than H_{cr}/H_c of either end-member. Such behavior is characteristic of bimodal mixtures in which H_{cr} is largely determined by the hard (SD) phase and H_c by the soft (MD) phase. The only mixture that could not be modeled by linear or nonlinear parameter theory was MD plus bacterial SD. The bacterial SD hysteresis loop descends almost vertically at $-H_c$ because of the extremely narrow range of particle sizes and coercivities. In general, linear and nonlinear parameter mixing models are adequate if only an approximate fit to real data is needed. An inversion method using complete magnetization curves as end-member basis functions is preferable as an unmixing technique. However, comparison of measured data to type curves, for example, on a Day plot, gives a quick indication of what end-member phases might be involved in the mix and provides additional insight before beginning an inversion.

Citation: Dunlop, D. J., and B. Carter-Stiglitz (2006), Day plots of mixtures of superparamagnetic, single-domain, pseudosingle-domain, and multidomain magnetites, *J. Geophys. Res.*, *111*, B12S09, doi:10.1029/2006JB004499.

1. Introduction

[2] An important problem in rock magnetism is finding the proportions of phases in a mixture from hysteresis or other magnetic measurements. In the simplest situation, the mixture consists of two phases with known properties. *Carter-Stiglitz et al.* [2001] have devised and tested a singular value decomposition method to ''unmix'' the hysteresis loop of the mixture, using the end-member hysteresis loops as basis functions. It often happens, particularly for data from the literature, that complete hysteresis loops are not available but only values of the hysteresis parameters M_s (saturation magnetization), M_{rs} (saturation remanent magnetization) and H_c (coercive force) from the induced magnetization loop and H_{cr} (remanent coercive force) from the remanent hysteresis loop. *Dunlop* [2002a, 2002b] derived and tested equations that combine end-member parameters to predict the parameters of the mixture. The inverse ''unmixing'' problem can be solved using the same equations.

[3] One application of *Dunlop*'s [2002a] method is in predicting values of the parameter ratios M_{rs}/M_s and H_{cr}/H_c and curves relating them on the Day plot [*Day et al.*, 1977]. The ratios are diagnostic of domain state: superparamagnetic (SP), stable single-domain (SD), pseudosingle-domain (PSD), multidomain (MD), or a mixture of these. The boundaries between regions on the Day plot are specified by: $M_{rs}/M_s \geq 0.5$ and $1 \leq H_{cr}/H_c \leq 2$ for SD grains; $0.02 \leq M_{rs}/M_s \leq 0.5$ and $1 \leq H_{cr}/H_c \leq 5$ for PSD magnetites and

[1]Geophysics, Physics Department, University of Toronto, Toronto, Ontario, Canada.
[2]Institute for Rock Magnetism, University of Minnesota, Minneapolis, Minnesota, USA.

0148-0227/06/2006JB004499$09.00

Table 1. Measured and Calculated Hysteresis Parameters of the End-Member Phases

Sample	M_{rs}, kA/m	M_{rs}/M_s	$\mu_0 H_c$, mT	$\mu_0 H_{cr}$, mT	H_{cr}/H_c	χ, MA m^{-1} T^{-1}	χ_r, MA m^{-1} T^{-1}
Ferrofluid		0.006	0.22	6.4	29.4		
MV1H	239	0.498	46.0	52.5	1.14	5.20	4.55
CS912	202	0.421	32.5	37.3	1.15	6.215	5.415
GC69B4	209	0.435	50.1	73.8	1.47	4.17	2.83
3006	99.4	0.207	24.4	49.8	2.04	4.07	2.00
041183[a]	23.0	0.048	5.56	26.1	4.69	4.14	0.88
041183[b]	24.5	0.051	6.36	25.45	4.00	3.85	0.96

[a]Parameter values used in calculations for physical mixtures.
[b]Parameter values used in calculations for numerical mixtures.

many mixtures of SD and MD grains; $M_{rs}/M_s \leq 0.02$ and $H_{cr}/H_c \geq 5$ for MD magnetites; and $M_{rs}/M_s \geq 0.1$ with $H_{cr}/H_c \gg 2$ (occasionally up to 50) for SP plus SD mixtures [*Dunlop*, 2002a, Figure 2].

[4] The purpose of this paper is to test to what extent approximations made in the theory compromise the general application of *Dunlop*'s [2002a] method. We do this by comparing theoretical predictions with the actual parameters from complete hysteresis loops of numerical or physical mixtures of SD with SP, PSD and MD magnetites.

2. Theory

[5] If both end-members are magnetite, M_s is constant (480 kA/m) for all mixtures. M_{rs}/M_s of the mixture is a linear combination of the M_{rs}/M_s values of the end-members:

$$M_{rs}/M_s = f_1(M_{rs}/M_s)_1 + f_2(M_{rs}/M_s)_2, \quad (1)$$

where f_1, f_2 are the volume fractions of phases 1 and 2. If phase 2 is SP, with $M_{rs} = 0$, M_{rs}/M_s of the mixture is simply equal to f_1 $(M_{rs}/M_s)_1$.

[6] H_{cr} and H_c of the mixture are nonlinear combinations of H_{cr} and H_c values of the end-member phases. To make the problem tractable, *Dunlop* [2002a] assumed that the descending hysteresis loop between M_{rs} and $-H_c$ (or the ascending loop between $-M_{rs}$ and H_c) is linear, with a slope $\chi = M_{rs}/H_c$. Similarly the descending remanent hysteresis loop between M_{rs} and $-H_{cr}$ or the ascending loop between $-M_{rs}$ and H_{cr} was assumed to be linear, with a slope $\chi_r = M_{rs}/H_{cr}$. Then for the coercive forces of the mixture, we have:

$$H_c = \left[f_1\chi_1(H_c)_1 + f_2\chi_2(H_c)_2\right]/(f_1\chi_1 + f_2\chi_2) \quad (2)$$

$$H_{cr} = \left[f_1\chi_{r1}(H_{cr})_1 + f_2\chi_{r2}(H_{cr})_2\right]/(f_1\chi_{r1} + f_2\chi_{r2}). \quad (3)$$

Equations (2) and (3) will be referred to as the "linear theory" because they assume linearity of segments of the hysteresis loops, although the equations themselves are not linear.

[7] A "nonlinear theory" for H_{cr} of SD plus MD mixtures was also proposed, based on a mathematical model of the MD remanent hysteresis curve suggested by *Nagata and Carleton* [1987]. In this case we have

$$f_{MD}(M_{rs})_{MD}\left\{1 - \left[(H_{cr})_{MD}/H_{cr}\right]\right\} + f_{SD}(M_{rs})_{SD}\left\{\left[H_{cr}/(H_{cr})_{MD}\right] - 1\right\} = 0. \quad (4)$$

This nonlinear equation for H_{cr} must be solved by trial and error.

[8] SP grains are in thermal equilibrium with an applied magnetic field H for ordinary times and temperatures. They have SD structure but, effectively, have no anisotropy to pin the magnetization M:

$$M = M_s L(\alpha) = M_s(\coth\ \alpha - 1/\alpha), \alpha \equiv \mu_0 V M_s H/kT. \quad (5)$$

(In (5), $\mu_0 = 4\pi \times 10^{-7}$ H/m, V is grain volume, $k = 1.38 \times 10^{-23}$ J/K is Boltzmann's constant, and T is temperature.) In a mixture of SP and thermally stable SD grains, H_{cr} is equal to H_{cr} of the stable SD fraction because the SP grains have no remanence. However, H_c of the mixture is considerably reduced by the SP fraction. The Langevin function L(α) rises steeply and soon saturates as H increases. We therefore approximate (5) by an initial ramp with slope $\chi_{SP} = \mu_0 V M_s^2/3kT$ plus a saturation line, $M = M_s$. Different expressions for H_c apply in these two ranges. In the initial ramp region,

$$H_c = f_{SD}\chi_{SD}(H_c)_{SD}/(f_{SD}\chi_{SD} + f_{SP}\chi_{SP}), \quad (6)$$

whereas if H_c is above SP saturation, we have

$$H_c = \left[1 - (f_{SP}/f_{SD})/(M_{rs}/M_s)_{SD}\right](H_c)_{SD}. \quad (7)$$

Because χ_{SP} is $\gg \chi_{SD}$, H_c from (6) is usually $\ll (H_c)_{SD}$. This in turn produces values of $H_{cr}/H_c \gg (H_{cr}/H_c)_{SD}$. These high H_{cr}/H_c values are characteristic of SP plus SD mixtures [*Dunlop*, 2002a, Figure 2].

[9] Bimodal SD plus MD mixtures (used also to model PSD grains) have end-members with greatly contrasting values of χ, χ_r, H_{cr} and H_c. When H_{cr}/H_c values are calculated for the mixture by dividing the nonlinear equations (2) and (3), "anomalously" high H_{cr}/H_c values can result. In extreme cases, the H_{cr}/H_c value of the mixture is predicted to be greater than the H_{cr}/H_c values of either end-member [*Wasilewski*, 1973; *Day et al.*, 1977]. This is documented for experimental mixtures of phases with very different values of H_{cr} and H_c [*Day et al.*, 1977; *Parry*, 1982; *Dunlop*, 2002a, Figure 12] and is demonstrated by one of the SD plus MD mixtures studied in this paper.

3. Samples and Methods

[10] The end-member phases in the mixtures are ~0.1 wt% dispersions in CaF_2 of six different magnetites of widely varying grain sizes. Hysteresis parameters (Table 1) were measured with a vibrating sample magnetometer. The SP

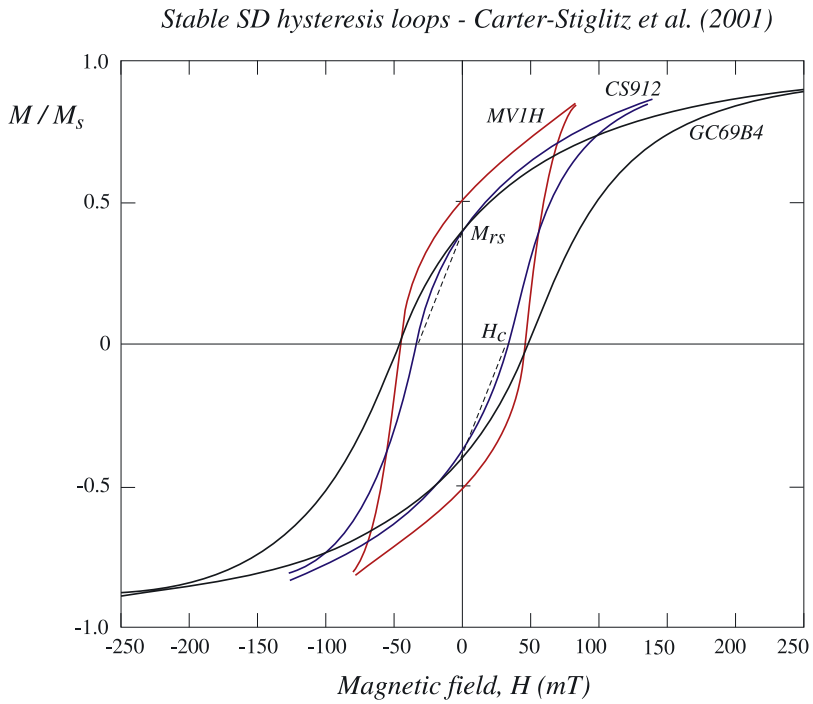

Figure 1. Measured hysteresis loops for the three single-domain end-member magnetites: MV1H (bacterial, magnetosome chains), CS912 (natural, volcanic), and GC69B4 (synthetic, glass matrix). The linear approximation (dashed line) used in modeling is compared to the data for CS912.

phase is Ferrofluid®, a colloidal suspension of ≈10 nm magnetite crystals [*Carter-Stiglitz et al.*, 2001] with very low M_{rs}/M_s (0.006) and very high H_{cr}/H_c (≈30). Wright Company synthetic magnetites 3006 and 041183 are the PSD and MD phases. Grain sizes are 1.06 ± 0.71 μm for 3006 and 18.3 ± 12.0 μm for 041183 [*Yu et al.*, 2002]. Hysteresis parameters are M_{rs}/M_s = 0.207, H_{cr}/H_c = 2.04 for 3006 and M_{rs}/M_s = 0.05, H_{cr}/H_c = 4.0–4.7 for 041183.

[11] Three magnetites have grain sizes in the stable SD range [*Enkin and Williams*, 1994; *Fabian et al.*, 1996; *Newell and Merrill*, 1999]. MV1H contains magnetotactic bacterial cells with intact chains of magnetite crystals [*Moskowitz et al.*, 1989, 1993]. Individual magnetosomes in the chains have dimensions averaging 35 × 35 × 53 nm. CS912 is a sample of the Tiva Canyon Tuff from Yucca Mountain, Nevada containing ≈100 nm magnetite crystals [*Schlinger et al.*, 1991]. GC69B4 is a glass ceramic sample whose magnetite crystals are ≤100 nm in size [*Worm and Markert*, 1987]. The crystals are well dispersed and noninteracting in all three samples judging by values of *R* (crossover between isothermal remanence acquisition and demagnetization curves) very close to 0.5 [*Cisowski*, 1981]. Hysteresis parameters are those of isolated SD grains: M_{rs}/M_s = 0.498, 0.421 and 0.435, H_{cr}/H_c = 1.14, 1.15 and 1.47, respectively.

[12] Three sets of mechanical mixtures were made, combining MV1H with Ferrofluid, 3006 and 041183 magnetites in volume fractions 0:1, 0.1:0.9, . . ., 0.9:0.1, 1:0. A few additional mixtures were made with ratios of 0.05:0.95 and 0.95:0.05. Physical mixtures could not be made using the other two SD end-members, CS912 and GC69B4, because the magnetite particles are in a rock or glass matrix. Instead measured hysteresis and remanent hysteresis loops of CS912 and GC69B4, scaled down appropriately, were added point by point to complementary downscaled loops for 041183. These SD plus MD "numerical mixtures" were calculated in proportions ranging from 0:1 to 1:0 in 10% increments. Measured loops of MV1H, CS912 and GC69B4 are compared in Figure 1.

[13] Table 1 lists the derived parameters $\chi = M_{rs}/\mu_0 H_c$ and $\chi_r = M_{rs}/\mu_0 H_{cr}$ used in calculations using equations (2), (3) and (6). An additional unlisted parameter (needed in equation (6)) is χ_{SP}, which we calculated from the initial slope of equation (5). Because the Ferrofluid particles are so small (10 nm), the SP susceptibility is relatively modest: χ_{SP} = 25. Our calculations were carried out in cgs units, in which χ_{SP}, χ and χ_r are dimensionless and have values 10 times smaller than the SI values in Table 1.

4. Results

[14] We obtained the best fit to the Day plot data for mechanical mixtures of MV1H and Ferrofluid (SD plus SP) by assuming 8 nm rather than 10 nm SP particles (Figure 2, left), which changed χ_{SP} from 25 to 10. This reduction in χ_{SP} may reflect interactions between particles rather than an actual size difference. The SD plus 10 nm SP model curve (not shown) falls to the upper right of the data, at a distance about equal to that of the SD plus 8 nm SP curve for large SP fractions (>70%) but much farther from the data than the 8 nm curve for SP fractions<70%. Measured and predicted M_{rs}/M_s values agree well for all mixtures except the one with 95% Ferrofluid/SP magnetite. Experimentally M_{rs}/M_s = 0.044, almost the same as M_{rs}/M_s = 0.048 for the 90% mixture and much greater than the predicted M_{rs}/M_s = 0.025. H_{cr}/H_c data are not so well accounted for. Predicted values for 8 nm SP mixtures are significantly higher than

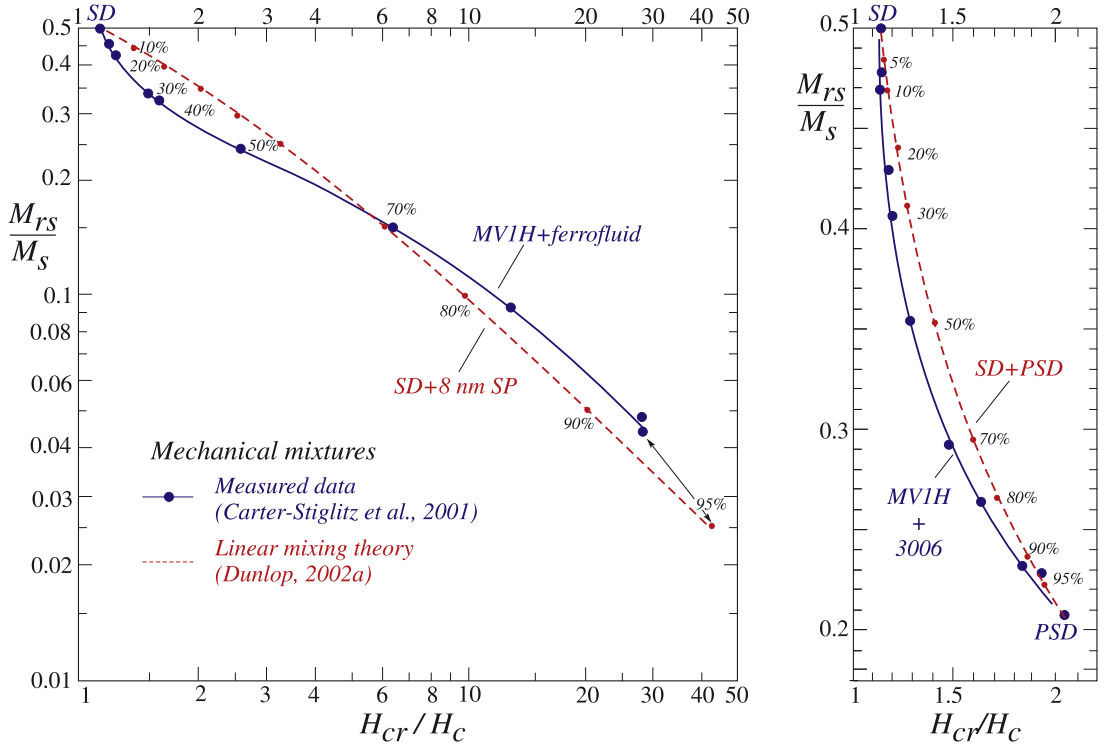

Figure 2. Measured M_{rs}/M_s and H_{cr}/H_c data for mixtures of MV1H (SD) with Ferrofluid (SP) and with Wright 3006 (PSD) magnetites compared to the predictions of linear mixing theory. Numbers along the curves are percentages of the SP or PSD phase.

experimental ones for $f_{SP} \leq 0.5$ but fall short for $f_{SP} \geq 0.8$. The sigmoidally shaped experimental curve resembles theoretical curves which combine calculations using equation (7) at small f_{SP} and equation (6) at large f_{SP} [*Dunlop*, 2002a, Figure 2]. For a χ_{SP} as small as 10, however, we are in the initial ramp part of the Langevin function (equation (6)) for all f_{SP}. The theoretical curve is then uninflected and convex up. The same discrepancy was seen in mixtures of Ferrofluid and Wright 3006 magnetites (data of B. Moskowitz [see *Dunlop*, 2002a, Figure 4]).

[15] Figure 2 (right) compares data for MV1H + 3006 mechanical mixtures with the predictions of linear SD plus PSD mixing theory (equations (1)–(3)). Theoretical and measured M_{rs}/M_s values agree well for all mixtures. The agreement between experimental and predicted H_{cr}/H_c results is acceptable, although the differences amount to 15% of the total range (1.14–2.04) for the 50:50 and 30:70 mixtures.

[16] More striking differences are seen when the range of H_{cr}/H_c data is larger. Modeling for mixtures of CS912 and 041183 gives an almost perfect fit to the M_{rs}/M_s and H_{cr}/H_c values for numerically combined loops (Figure 3). However, linear mixing theory fails to match H_{cr}/H_c values determined from numerically mixed GC69B4 and 041183 loops (Figure 4). Nonlinear theory (using equation (4) for H_{cr}) comes closer to fitting the results but does not explain the "anomalous" H_{cr}/H_c value for $f_{MD} = 0.9$, which is greater than H_{cr}/H_c for the pure MD end-member. Finally, both linear and nonlinear mixing theories (equations (3) and (4) for H_{cr}) give simple uninflected curves that bear little resemblance to the strongly inflected curve measured for MV1H + 041183 physical mixtures (Figure 5).

[17] Trends in the H_{cr} and H_c results separately are shown for GC69B4 + 041183 mixtures in Figure 6. The H_c results are explained almost perfectly by equation (2), but linear theory (equation (3)) does not even approximately match the H_{cr} numerical data. Nonlinear theory (equation (4)) comes closer but the differences are significant when $f_{SD} \leq 0.3$.

[18] Differences between predicted and observed/calculated values of H_c can be important in some cases (Figure 7). Agreement is acceptable for the CS912 and GC69B4 mixtures, but the MV1H plus MD data deviate in a major way from the predictions of equation (2) when the SD fraction is large ($f_{SD} \geq 0.4$). The assumption of linearity in the hysteresis curve between M_{rs} and $-H_c$ is conspicuously violated for MV1H (see Figure 1).

5. Discussion

[19] Linear and nonlinear mixing models that use only the hysteresis parameters of the end-member phases are attractive because they require minimal input information. However, they give fits of varying quality to experimental mixing curves or curves based on weighted sums of end-member hysteresis loops. MV1H was the SD end-member in three mixtures, with Ferrofluid (SP), 3006 (PSD) and 041183 (MD) (Figures 2 and 5). The theoretical fits were acceptable for the PSD mixture, where end-member parameters do not differ too greatly from each other, but unconvincing for the SP and MD mixtures, which have greater contrasts in the end-member parameters H_c, H_{cr}, χ_r and χ_{SP}.

[20] The SD plus SP model curve in Figure 2 depends critically on the size of the Ferrofluid magnetite particles.

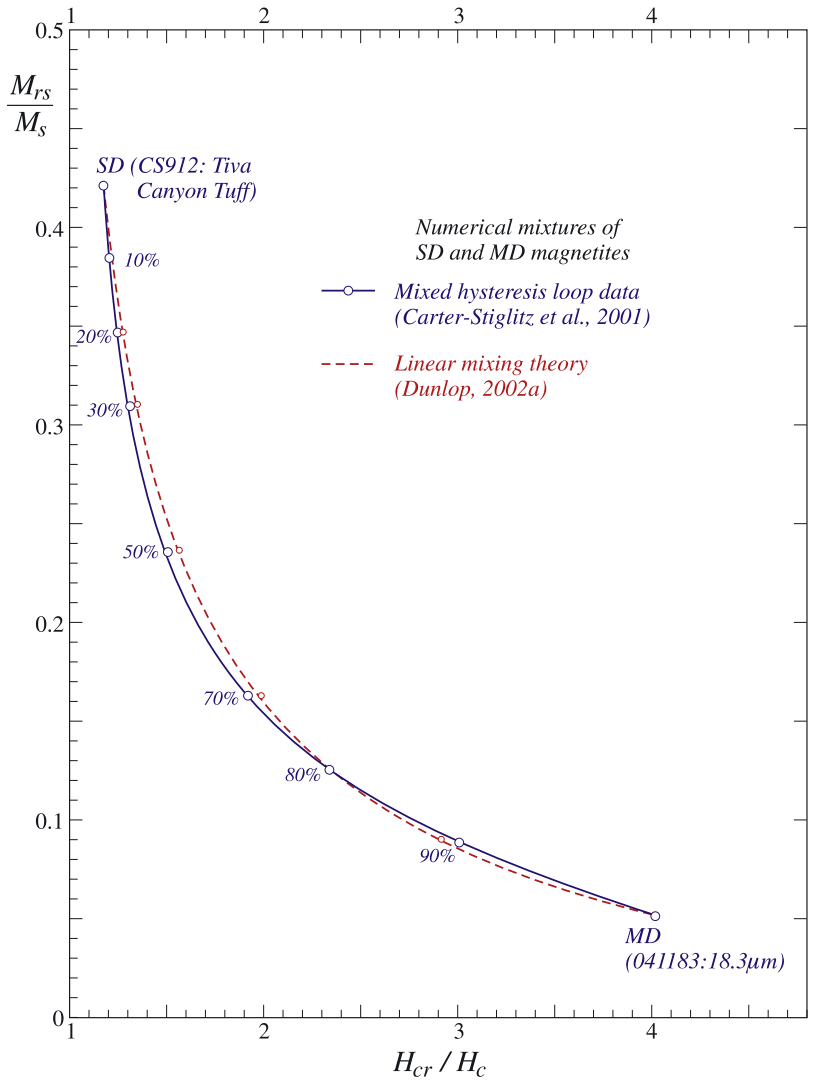

Figure 3. M_{rs}/M_s and H_{cr}/H_c data obtaining by mixing measured hysteresis loops of CS912 (SD) and Wright 041183 (MD) in varying proportions (numbers along curves) compared to the predictions of linear mixing theory.

The initial slope of the Langevin function (equation (5)) is very sensitive to V: for 10 nm particles, χ_{SP} is 2.5 times larger than for 8 nm particles. Using a smaller χ_{SP} that is closer to χ of MV1H allowed us to achieve a better average fit but we sacrificed the inflected shape characteristic of larger SP particle sizes (this shape results from using equation (7) when f_{SP} is small and equation (6) for large f_{SP}). A distribution of sizes instead of the single SP particle size we assumed might permit a closer overall fit.

[21] It is enlightening to compare the quality of fits in the three SD plus MD mixtures. When the SD end-member is CS912, the agreement of linear theory with mixed hysteresis loop data is well-nigh perfect (Figure 3). There is comparatively good linearity in the CS912 hysteresis loop between M_{rs} and $-H_c$ (Figure 1) as well as in the remanent hysteresis loop between M_{rs} and $-H_{cr}$ (Figure 8). The 041183 hysteresis loop is ramp-like as a result of self-demagnetization and is adequately linear in fields as large as 32.5 mT, the coercive force of CS912. MD remanent hysteresis loops depend less on self-demagnetization than on the distribution of microcoercivities. This distribution is fairly uniform over the range between H_{cr} of 041183 (25.45 mT) and H_{cr} of CS912 (37.3 mT). Linear theory therefore works well for H_{cr} of the mixtures (equation (3)) as well as for H_c (equation (2)).

[22] For the GC69B4 + 041183 mixtures (Figures 4 and 6), linearity of the SD hysteresis curve (Figure 1) is again adequate to produce a good fit between linear theory and the H_c data. However, the H_{cr} values of the end-members are now rather different (25.45 and 73.8 mT). A linear projection of the remanent hysteresis curve of 041183 from H_{cr} to almost $3H_{cr}$ no longer matches the real curve over the same range (Figure 8) and equation (3) fails. The curvature of the real loop is well matched (although not perfectly) by the model of *Nagata and Carleton* [1987] and equation (4) gives a reasonable match to the H_{cr} values of the mixtures up to $f_{MD} = 0.8$ (Figures 4 and 6).

[23] Theoretical fits disagree with mechanical mixture data for MV1H + 041183 no matter what equations are used. The H_{cr} values of the end-members differ by only a factor 2 (26.1 and 52.5 mT), so that the MD remanent hysteresis curve is not being projected unacceptably far

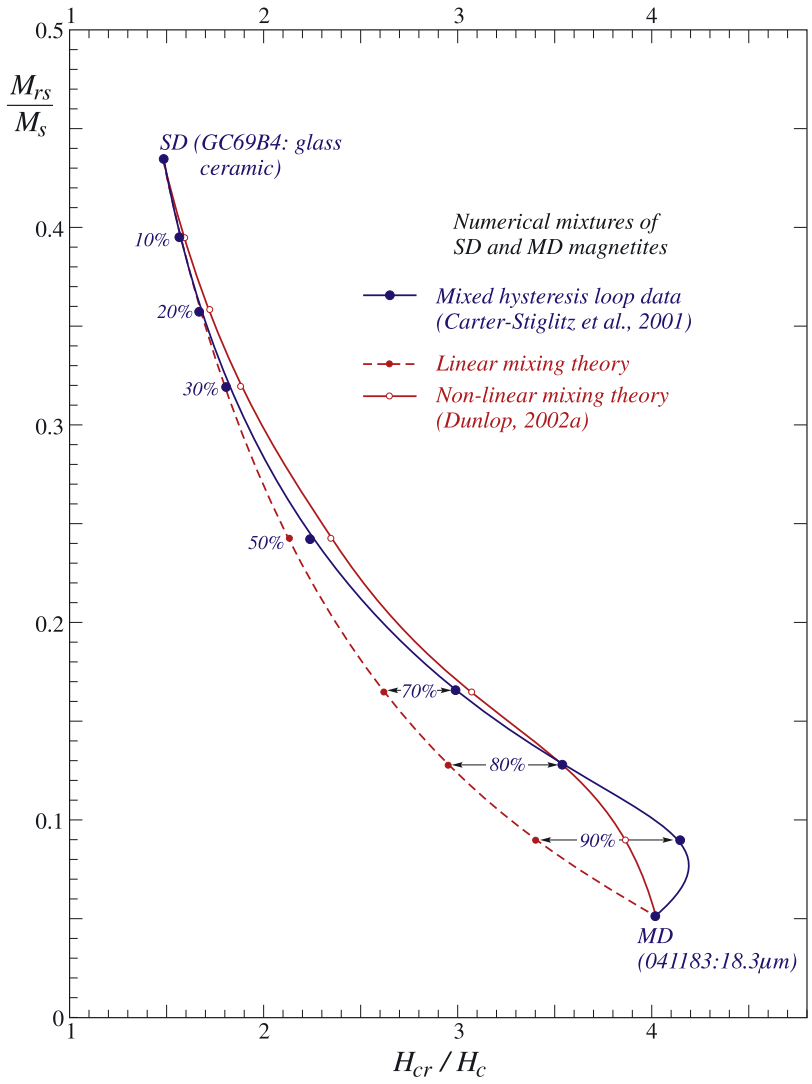

Figure 4. M_{rs}/M_s and H_{cr}/H_c data obtaining by mixing measured hysteresis loops of GC69B4 (SD) and Wright 041183 (MD) in varying proportions (numbers along curves) compared to the predictions of linear and nonlinear mixing theories. Nonlinear theory (equation (4)) matches the data well except for the 90% MD mixture.

beyond its linear region. As evidence of this, linear and nonlinear theories are in quite close agreement (Figure 5). Unfortunately neither curve matches the data. Figure 7 suggests that failure of equation (2) to match the experimental H_c data for MV1H is the cause. It is clear from Figure 1 that the MV1H hysteresis curve is grossly nonlinear between M_{rs} and $-H_c$, so that equation (2) is bound to fail. The MV1H remanent hysteresis curve is similarly nonlinear between M_{rs} and $-H_c$ (Figure 8) and so equation (3) fails.

[24] For a successful application of equations (2)–(4), the first step is to examine the hysteresis and remanent hysteresis loops of both end-members for linearity. The MV1H hysteresis loop (Figure 1) has a very sharp descent at $H = -H_c$, typical of a narrow distribution of microcoercivities. Magnetotactic bacteria produce magnetite crystals of nearly identical sizes (in the SD range, which is narrow for magnetite) in chains of similar lengths. While this serves the needs of the bacteria well, it results in a grossly nonlinear descending loop segment between M_{rs} and $-H_c$ and invalidates our theoretical approach. We would expect a similar failure if attempting to model mixtures involving synthetic particles used for magnetic recording because they too are designed to have a single switching field.

[25] Our most successful SD plus MD mixtures used CS912, which contains a distribution of particle sizes from the stable SD range downward into SP sizes [*Worm and Jackson*, 1999; *Jackson et al.*, 2004]. The distribution of microcoercivities is fairly limited, the loop for CS912 closes around 125 mT, compared to 80 mT for MV1H, but the coercivities are quite uniformly distributed over the entire range, unlike those of MV1H, giving a quasi-linear descent from M_{rs} to at least $-2H_c$ (Figure 1). Mixtures with the glass ceramic sample GC69B4 as the SD end-member were also successfully modeled (H_c data, Figure 6). In this case, the descending loop is about as linear as that of CS912 but does not close until ≈200 mT (Figure 1), indicating a broader distribution of coercivities and particle sizes/shapes.

[26] Given the mixed success of our modeling, why use parameter mixing theory at all? If complete end-member

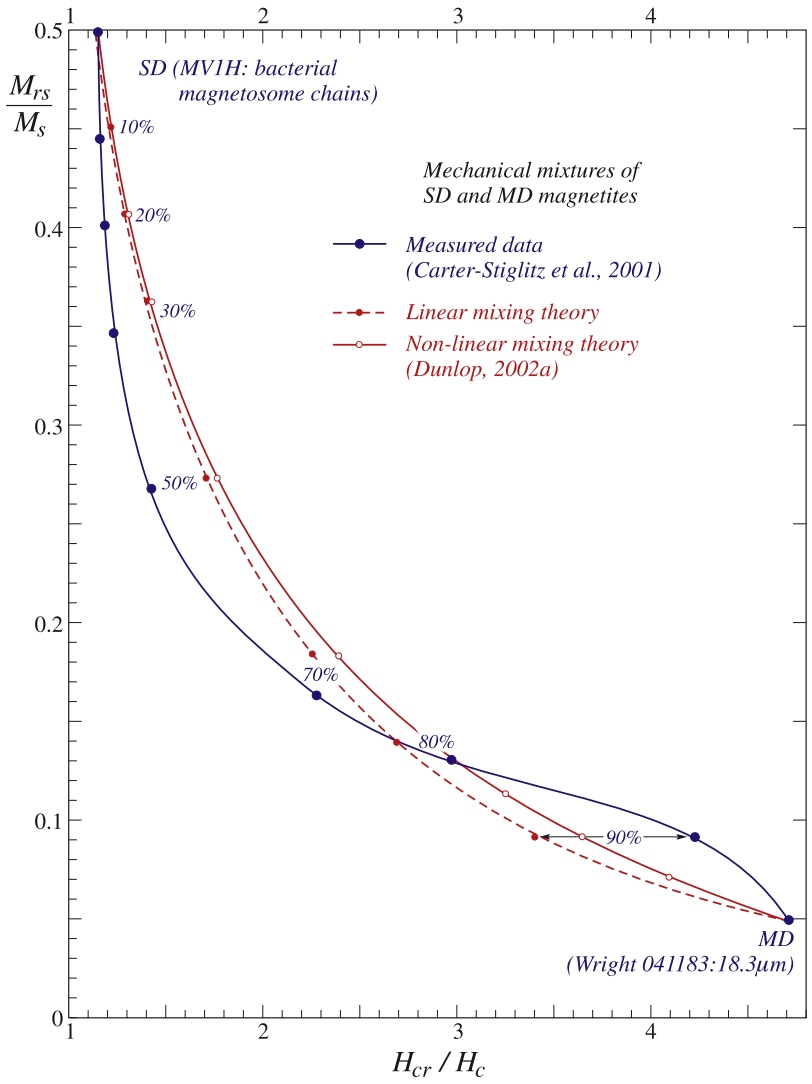

Figure 5. Measured M_{rs}/M_s and H_{cr}/H_c data for mixtures of MV1H (SD) with Wright 041183 (MD) magnetites compared to the predictions of linear and nonlinear mixing theories. Agreement is poor for all mixtures and both theories.

loops (remanent as well as induced) are known, it makes sense to mix entire loops and not to rely on the parameters M_{rs}, H_c and H_{cr}, which contain only a limited indication of loop shapes. Generally, however, we must deal with the mixtures nature has prepared, with only a limited knowledge of the end-member properties (or even what phases are mixed). Assembling a complete set of possible phases and their characteristic loops or basis functions is a formidable task because of the many degrees of freedom: M_s values; basic domain states; variations of remanence and average coercivity with grain size and shape within those domain categories; narrow versus wide distributions of size, shape, coercivity and remanence; interactions, including but not limited to interactions among particles in chains and other assemblages; and self-demagnetizing fields, which result from interaction among domains in PSD and MD grains and change in importance depending on magnetization level, i.e., throughout the hysteresis process.

[27] For practical reasons, we cannot cover all possibilities, even with an extensive catalog of representative hysteresis and remanent hysteresis loops. As a first cut, and to establish simple "type curves" for the Day plot (and other presentations of hysteresis data, such as an M_{rs}/M_s versus H_c diagram), simple parameter mixing models remain useful. If measured parameters disagree with binary mixture type curves, the mixtures may be bimodal, i.e., lacking any significant overlap in the distributions of end-member properties, or more than two phases may be mixed. For example, on the basis of trends of data on the Day plot, *Dunlop et al.* [2006] have documented mixtures of varying proportions of two types of magnetite in biotite grains, one occurring as small inclusions limited in size by exfoliation galleries within the host biotite and the other as much larger crystals at the edges of biotite grains. Many other examples, taken from published studies, are discussed by *Dunlop* [2002b].

6. Conclusions

[28] We have tested the effectiveness of using only a few hysteresis parameters instead of complete hysteresis curves

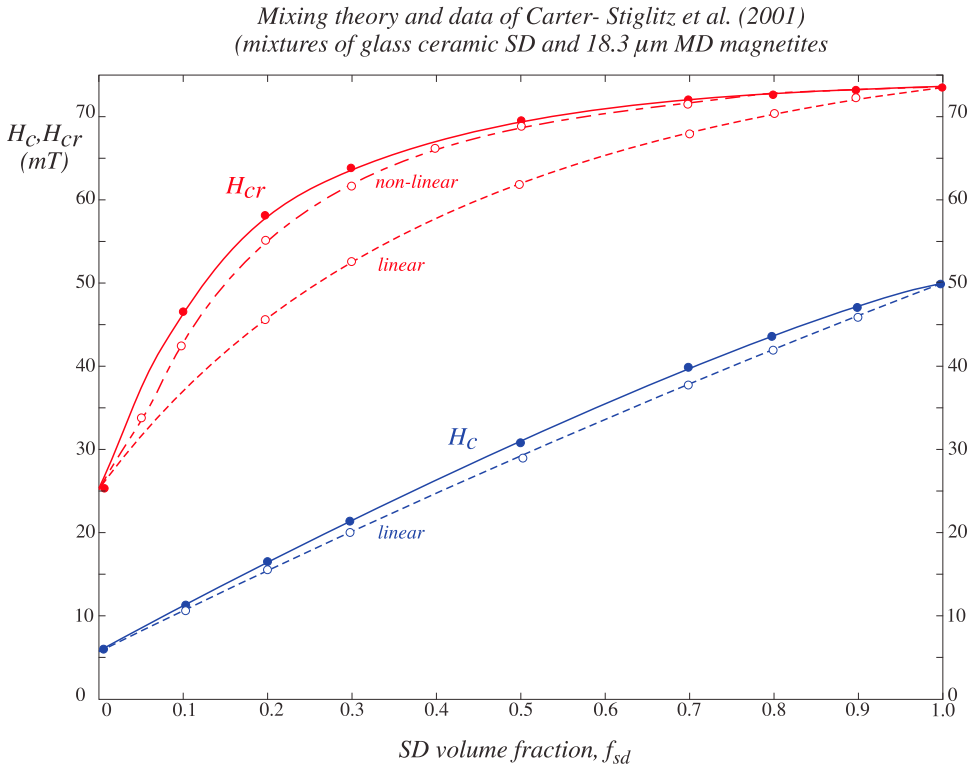

Figure 6. H_{cr} and H_c data obtaining by mixing measured hysteresis loops of GC69B4 (SD) and Wright 041183 (MD) in varying proportions compared to the predictions of linear and nonlinear mixing theories. Nonlinear theory (equation (4)) matches the H_{cr} data well except for small SD fractions ($f_{SD} \leq 0.3$).

in determining the proportions of the end-member phases in binary mixtures. Our end-members were six magnetites used earlier by *Carter-Stiglitz et al.* [2001] which have grain size and shape distributions that place them within the SP, thermally stable SD (three samples), PSD and MD ranges, respectively. The three SD magnetites have contrasting origins and properties: (1) bacterial magnetite crystals of a single size and coercivity, arranged in chains; (2) natural volcanic magnetites with a fairly narrow and uniform distribution of coercivities; and (3) synthetic magnetites precipitated in glass, with a broader coercivity distribution.

[29] Linearity is important. For our parameter mixing theory to work magnetization curves of the end-members must be acceptably linear between zero field and the largest coercive force H_c (typically the SD phase). Similarly, remanent hysteresis curves must be linear between zero and the maximum remanent coercive force H_{cr}. These requirements were met for three of our mixtures (SP plus bacterial SD, PSD plus bacterial SD, MD plus volcanic SD) judging by the good agreement between predicted and measured dependences of H_c, H_{cr} and the curve of M_{rs}/M_s versus H_{cr}/H_c (Day plot) on end-member concentrations. Our linear parameter mixing theory gave unacceptable fits to measured data or the results of numerically mixing entire hysteresis loops for the remaining two SD plus MD mixtures.

[30] A nonlinear approximation to remanent hysteresis curves (equation (4)) gave a closer although not perfect fit to the MD plus glass SD results (Figures 4 and 6). In this case, the H_{cr}/H_c results are "anomalous." H_{cr}/H_c for MD-rich mixtures is larger than H_{cr}/H_c of either the MD or SD end-members. Such behavior is characteristic of bimodal mixtures in which H_{cr} is largely determined by the hard (SD) phase and H_c by the soft (MD) phase [*Wasilewski*, 1973; *Day et al.*, 1977; *Parry*, 1982; *Dunlop*, 2002a, Figure 12]. The predicted curve almost, but not quite, matches the data for the 90% MD mixture.

[31] The only mixture that cannot be modeled at all by linear or nonlinear parameter theory is MD plus bacterial SD (Figure 5). The bacterial SD hysteresis loop (MV1H in Figure 1) descends almost vertically at $-H_c$ because the range of particle sizes and coercivities is extremely narrow. It is somewhat surprising that the pronounced nonlinearity of the MV1H curve between M_{rs} and $-H_c$ does not totally invalidate our modeling for the mixtures with SP and PSD magnetites (Figure 2). For that matter, the same segments of the volcanic SD and glass SD hysteresis loops (CS912 and GC69B4 in Figure 1) are not impressively linear either, although the range of coercivities is broader.

[32] We conclude that linear and nonlinear parameter mixing models (equations (1)–(4)) are more forgiving than anticipated if only an approximate fit to real data is needed. As the basis of an unmixing technique, an inversion method using complete magnetization curves as end-member basis functions is greatly to be preferred. However, comparison of measured data to type curves, for example on a Day plot, gives a quick indication of what end-members might be involved in the mix, which typically will involve three or four phases, not just two. This sort of comparison is particularly helpful for large data sets from closely related samples. There will inevitably be ambiguities but any

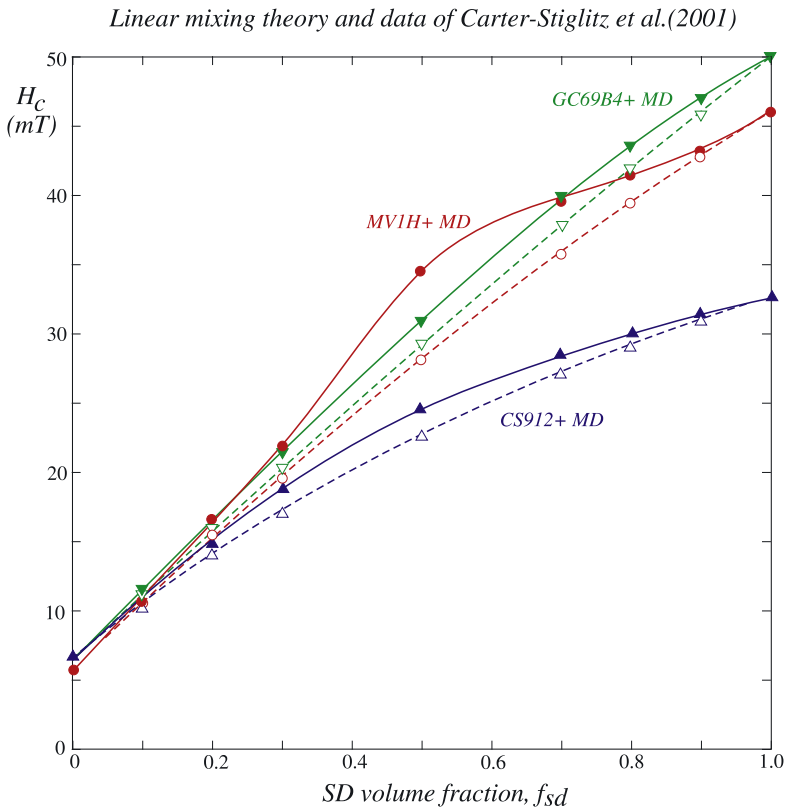

Figure 7. H_c data for mechanical or numerical mixtures of Wright 041183 (MD) in varying proportions with the three SD magnetites, compared to the predictions of linear mixing theory. Agreement is acceptable for the CS912 and GC69B4 mixtures, but there is gross disagreement for the MV1H plus MD mixture.

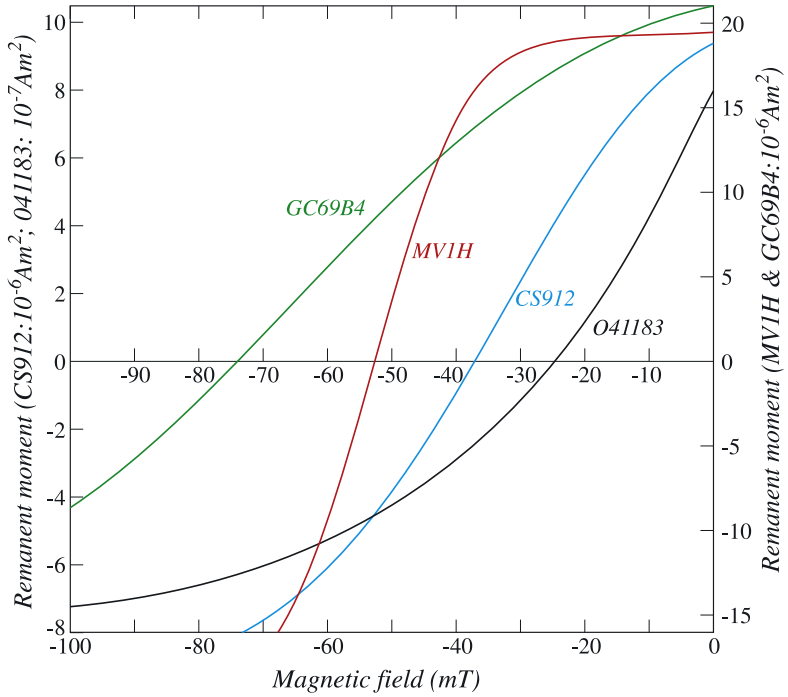

Figure 8. Partial remanent hysteresis curves ("DC demagnetization" curves) for the three SD samples and for MD sample 041183. The curves are acceptably linear between 0 and $-H_{cr}$ for CS912 and GC69B4, but for MV1H, coercivities below 40 mT are almost nonexistent, making the curve even more nonlinear than the descending hysteresis loop (Figure 1).

additional insight in the early stages is preferable to beginning an inversion blind.

[33] **Acknowledgments.** Results for mechanical and numerical mixtures were measured or computed at the Institute for Rock Magnetism, University of Minnesota, which is operated with support from the Keck Foundation and the Earth Sciences Division of NSF. We thank Bruce Moskowitz and Mike Jackson for their help. David Heslop provided a number of useful suggestions in his review of the paper. This is IRM contribution 0607. Numerical modeling at University of Toronto was supported by NSERC grant A7709 to D.J.D.

References

Carter-Stiglitz, B., B. Moskowitz, and M. Jackson (2001), Unmixing magnetic assemblages and the magnetic behavior of bimodal mixtures, *J. Geophys. Res.*, *106*, 26,397–26,411.

Cisowski, S. (1981), Interacting vs. non-interacting single domain behavior in natural and synthetic samples, *Phys. Earth Planet. Inter.*, *26*, 56–62.

Day, R., M. Fuller, and V. A. Schmidt (1977), Hysteresis properties of titanomagnetites: Grain size and composition dependence, *Phys. Earth Planet. Inter.*, *13*, 260–267.

Dunlop, D. J. (2002a), Theory and application of the Day plot (M_{rs}/M_s versus H_{cr}/H_c): 1. Theoretical curves and tests using titanomagnetite data, *J. Geophys. Res.*, *107*(B3), 2056, doi:10.1029/2001JB000486.

Dunlop, D. J. (2002b), Theory and application of the Day plot (M_{rs}/M_s versus H_{cr}/H_c): 2. Application to data for rocks, sediments, and soils, *J. Geophys. Res.*, *107*(B3), 2057, doi:10.1029/2001JB000487.

Dunlop, D. J., Ö. Özdemir, and D. G. Rancourt (2006), Magnetism of biotite crystals, *Earth Planet. Sci. Lett.*, *243*, 805–819.

Enkin, R. J., and W. Williams (1994), Three-dimensional micromagnetic analysis of stability in fine magnetic grains, *J. Geophys. Res.*, *99*, 611–618.

Fabian, K., A. Kirchner, W. Williams, F. Heider, T. Leibl, and A. Hubert (1996), Three-dimensional micromagnetic calculations using FFT, *Geophys. J. Int.*, *124*, 89–104.

Jackson, M., P. Sølheid. B. Carter-Stiglitz, and J. Rosenbaum (2004), Tiva Canyon Tuff (I): Superparamagnetic samples available, *Inst. Rock Magnet. Q.*, *14*(3), 1, 9–11.

Moskowitz, B. M., R. B. Frankel, D. A. Bazylinski, H. W. Jannasch, and D. R. Lovley (1989), A comparison of magnetite particles produced anaerobically by magnetotactic and dissimilatory iron-reducing bacteria, *Geophys. Res. Lett.*, *16*, 665–668.

Moskowitz, B. M., R. B. Frankel, and D. A. Bazylinski (1993), Rock magnetic criteria for the detection of biogenic magnetite, *Earth Planet. Sci. Lett.*, *120*, 283–300.

Nagata, T., and B. J. Carleton (1987), Magnetic remanence coercivity of rocks, *J. Geomagn. Geoelectr.*, *39*, 447–461.

Newell, A. J., and R. T. Merrill (1999), Single-domain critical sizes for coercivity and remanence, *J. Geophys. Res.*, *104*, 617–628.

Parry, L. G. (1982), Magnetization of immobilized particle dispersions with two distinct particle sizes, *Phys. Earth Planet. Inter.*, *28*, 230–241.

Schlinger, C. S., D. R. Veblen, and J. G. Rosenbaum (1991), Magnetism and magnetic mineralogy of ash flow tuffs from Yucca Mountain, Nevada, *J. Geophys. Res.*, *96*, 6035–6052.

Wasilewski, P. (1973), Magnetic hysteresis in natural materials, *Earth Planet. Sci. Lett.*, *20*, 67–72.

Worm, H.-U., and M. Jackson (1999), The superparamagnetism of Yucca Mountain Tuff, *J. Geophys. Res.*, *104*, 25,415–25,425.

Worm, H.-U., and H. Markert (1987), Magnetic hysteresis properties of fine particle titanomagnetites precipitated in a silicate matrix, *Phys. Earth Planet. Inter.*, *46*, 84–92.

Yu, Y., D. J. Dunlop, and Ö. Özdemir (2002), Partial anhysteretic remanent magnetization in magnetite: 1. Additivity, *J. Geophys. Res.*, *107*(B10), 2244, doi:10.1029/2001JB001249.

B. Carter-Stiglitz, Institute for Rock Magnetism, University of Minnesota, Minneapolis, MN 55455, USA.

D. J. Dunlop, Geophysics, Physics Department, University of Toronto, Toronto, ON, Canada M5S 1A7. (dunlop@physics.utoronto.ca)